Supplementary Information for

Membrane electrode assembly type cell designed for selective CO production from bicarbonate electrolyte and air containing CO_2 mixed gas

Akina Yoshizawa,[a] Manabu Higashi[a] Akihiko Anzai [a] and Miho Yamauchi[a,b,c,d]*

[a] Institute for Materials Chemistry and Engineering (IMCE), Kyushu University, Motooka 744, Nishi-ku, Fukuoka 819-0395, Japan.

[b] Advanced Institute for Materials Research (WPI-AIMR), Tohoku University 2-1-1 Katahira, Aoba-ku, Sendai 980-8577, Japan.

[c] Research Center for Negative Emissions Technologies (K-NETs), Kyushu University Motooka 744, Nishi-ku, Fukuoka 819-0395, Japan.

[d] International Institute for Carbon-Neutral Energy Research (WPI-I²CNER), Kyushu University Motooka 744, Nishi-ku, Fukuoka 819-0395, Japan.

*Corresponding author:

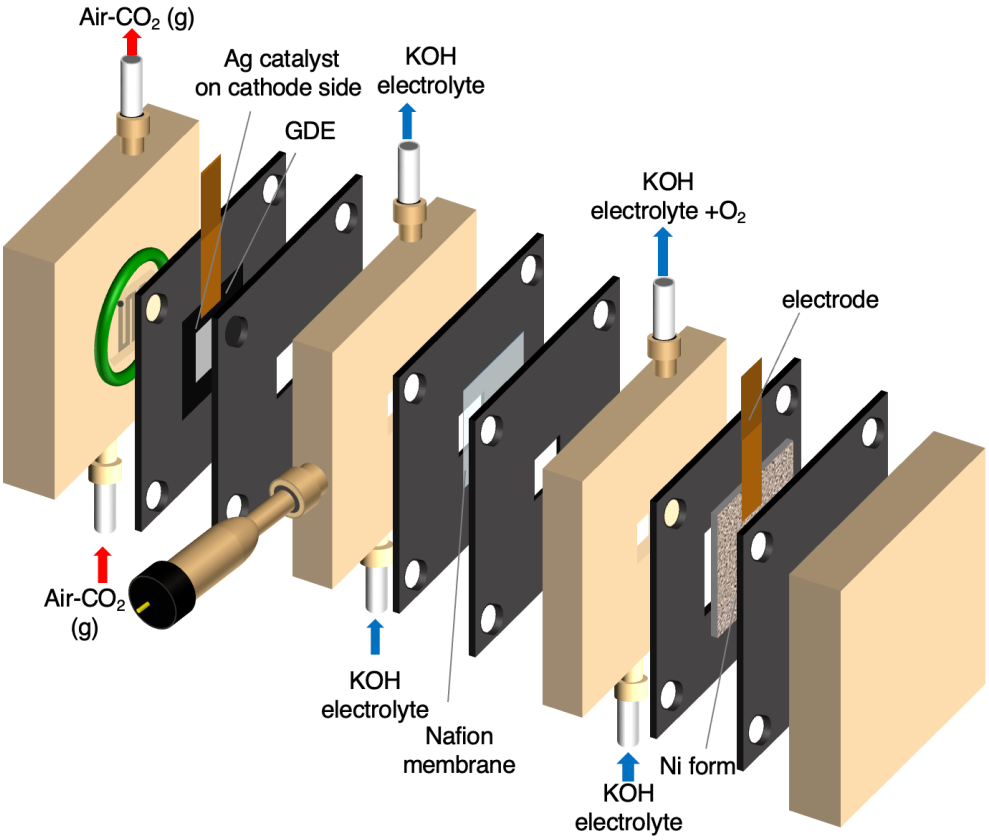

Figure S1. System configuration of conventional three-chamber cell.

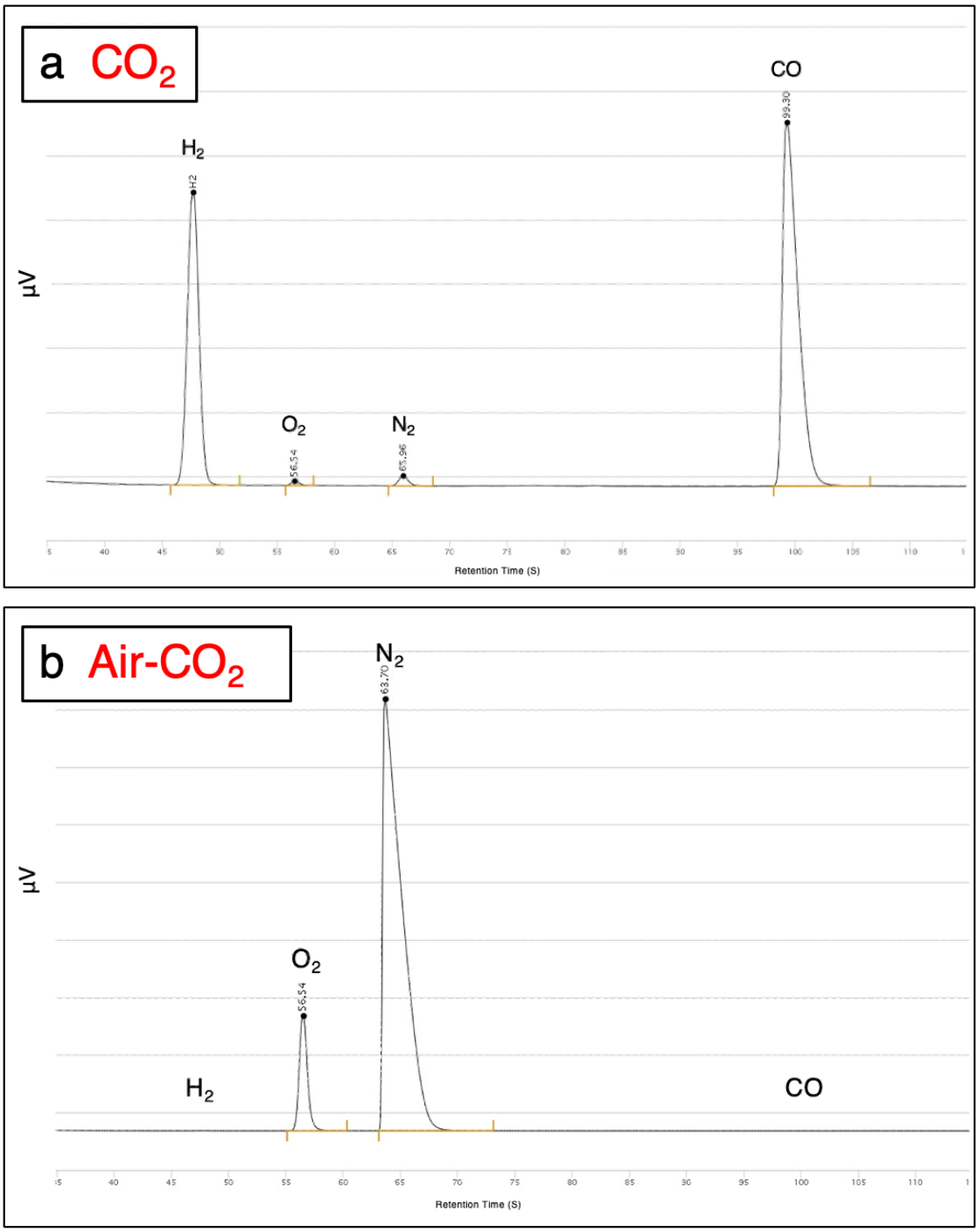

Figure S2. GC charts for the analysis of H_2 and CO produced in CO_2RR using (a) CO_2 and (b) Air-CO_2 on a conventional carbon based flow cell.

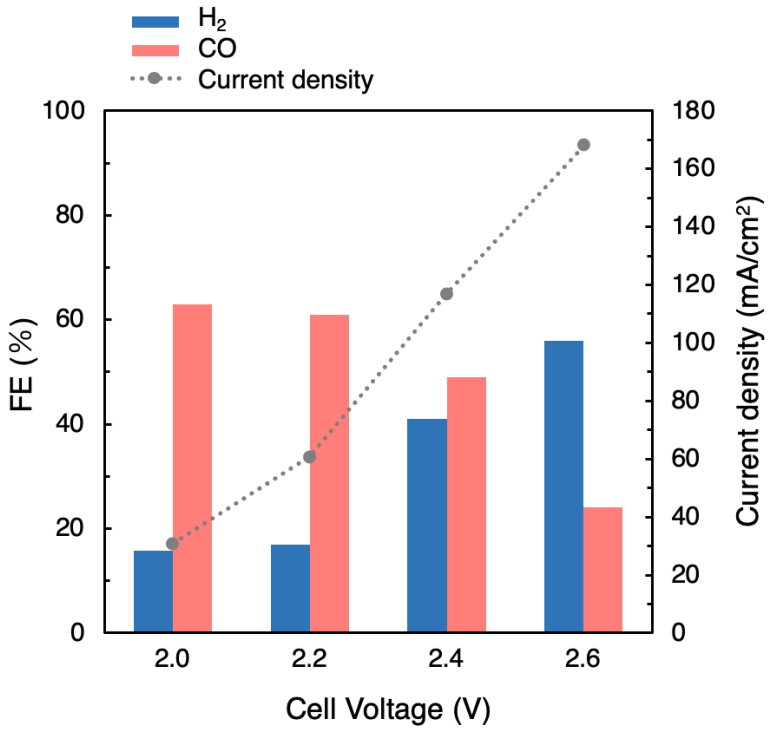

Figure S3. Faradaic efficiency (FE) in CO_2RR using 1.0 M BCS on a MEA cell with a carbon-based GDE.

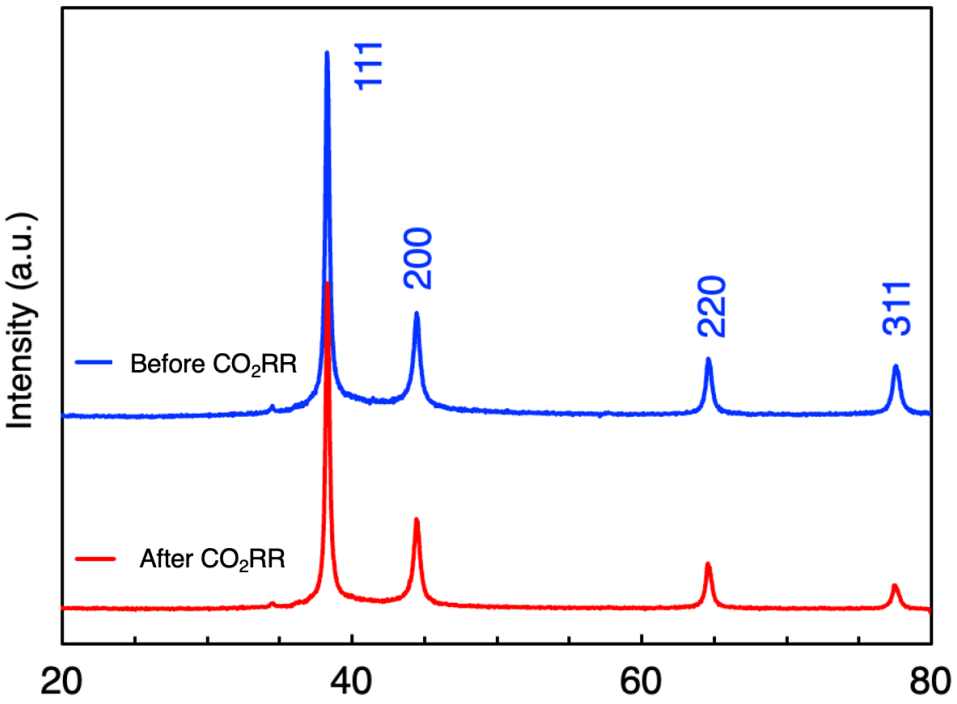

Figure S4. XRD diffraction patterns of the Ag NP catalyst on MEA before and after CO_2RR using 1.0 M BCS.

Table S1. Crystallographic data and Rietveld refinement parameters of the Ag NP catalyst on MEA before and after CO_2RR using 1.0 M BCS.

	before reaction	after reaction
crystal system	cubic	cubic
space group	Fm-3m	Fm-3m
a (Å)	4.088	4.089
V (Å^3)	68.32	68.40
crystallite size (nm)	26.4	25.2
T (K)	298	298
GOF	2.32	3.09
2θ range	30-80°	30-80°
wavelength (Å)	1.5405	1.5405

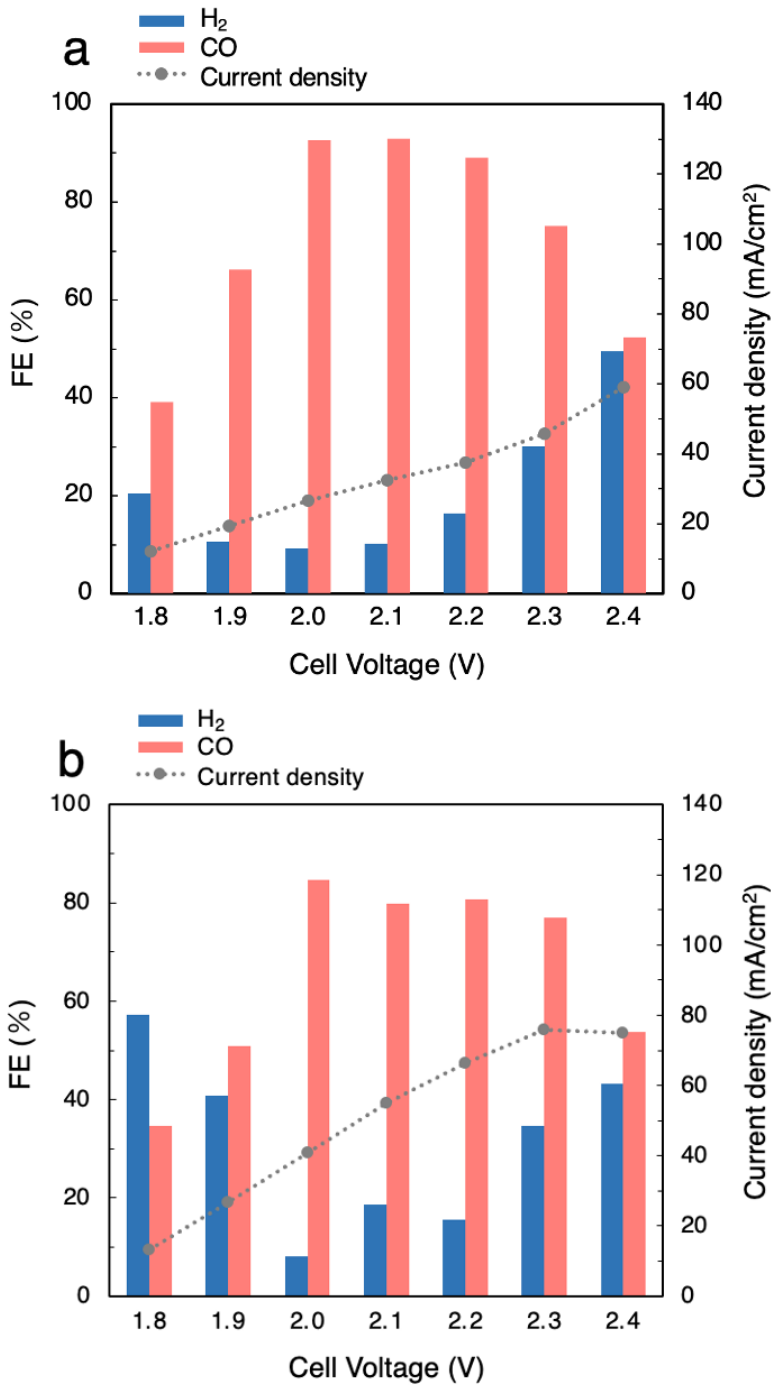

Figure S5. Faradaic efficiency (FE) and current density as a function of cell voltage for CO_2RR on Ag MEA-Cell in (a) 1.0M BCS and (b) 3.0M BCS.

Table S2. Electrolyte pH of the CO_2 capturing 1.0 M KOH.

gas	pH
1M KOH (before bubbling)	13.9
100% CO_2	7.55[a]
Air-CO_2	7.90[a]

[a] The pH of the 1M KOH solution after CO_2 capture. In a typical experiment, the pH was measured with 100 ml of KOH solution after purging with CO_2 containing gas at 30 sccm overnight.

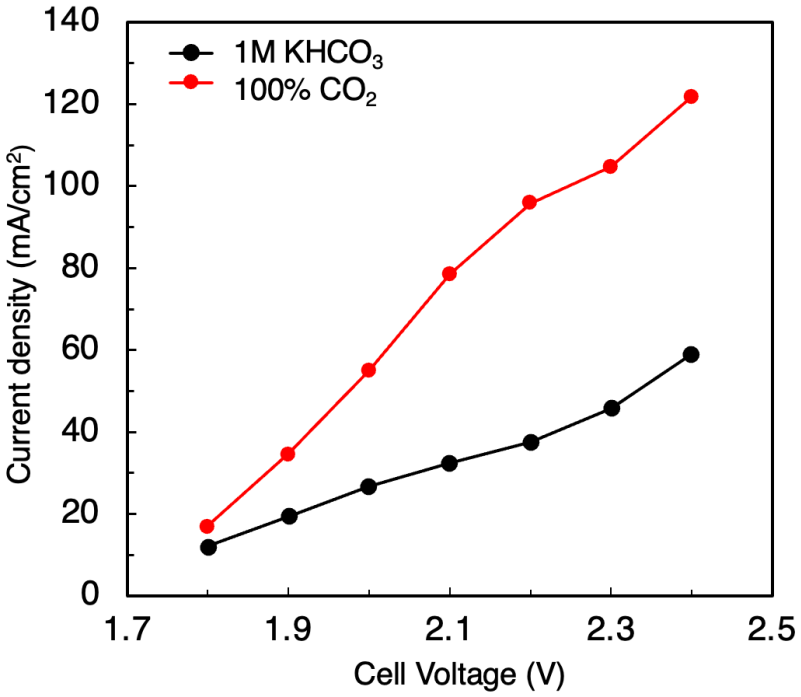

Figure S6. Current densities in CO_2RR using 1M BCS and 100 % CO_2 on Ag MEA-Cell.

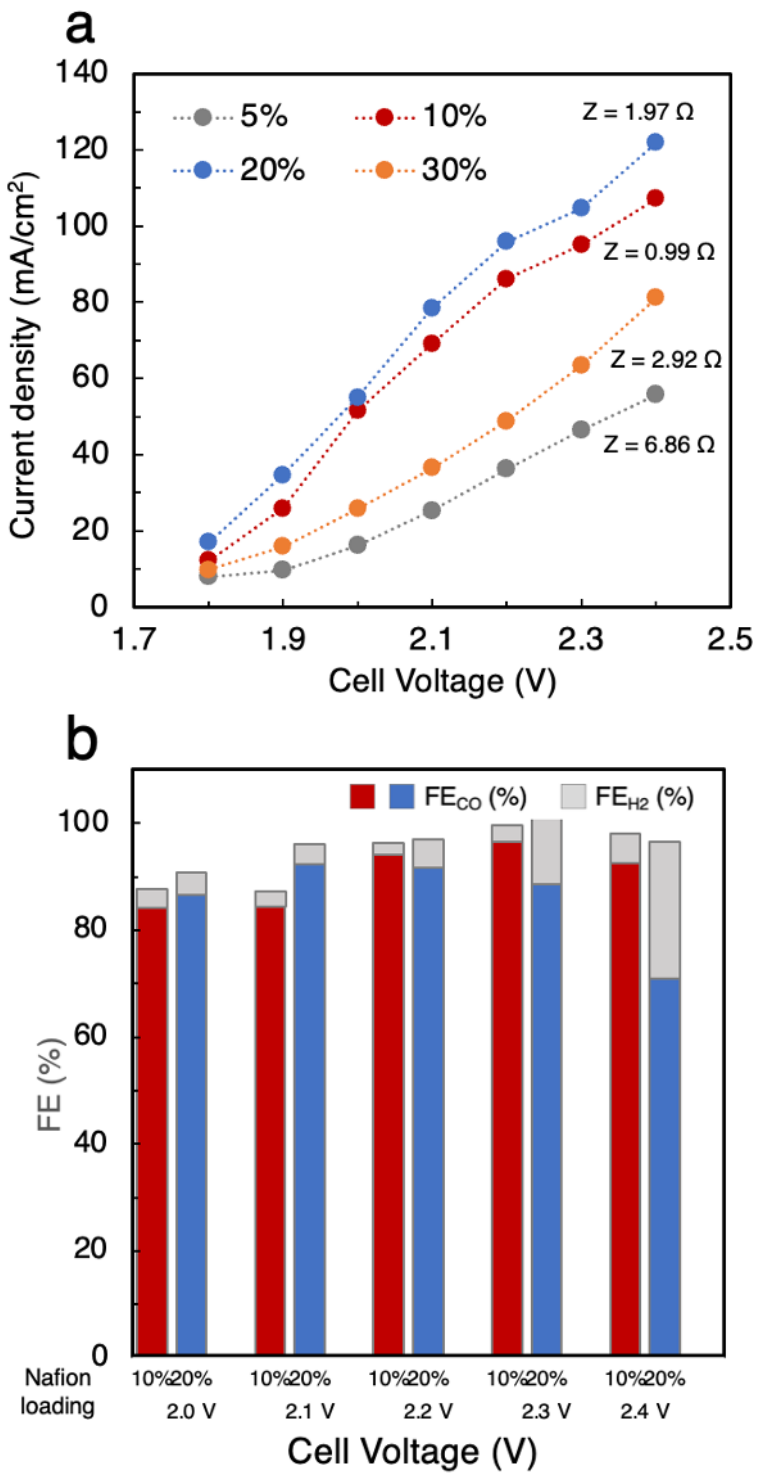

Figure S7. (a) Current-voltage curves and (b) Faradaic efficiency for CO (FE_{CO}) and H_2 production (FE_{H2}) in CO_2RR using pure CO_2 on Ag MEA-Cell with Ag catalysts including different ratio of Nafion solution.

The Nafion ionomers contained in the Ag catalyst ink enhance transport of CO_2 and H^+ at the catalytic sites.[45, 46] Thus, we examined the optimal loading amount of the Nafion ionomer from 5 to 30 % and found that MEAs with 10 to 20 wt% of Nafion loading to the amount of Ag on Ag-MEA (2.5 mg/cm^2) showed higher J values, which were almost double than those on MEAs with 5 or 30 wt% Nafion loading in the voltage range from 2.0 to 2.4 V (Figure S6a). The resistances for CO_2RR using MEAs with 5 or 30 % Nafion loading were measured to be 6.86 and 2.92 Ω, respectively, and the resistances were much higher than that with MEAs with 10 or 20 % Nafion loading (0.99 and 1.97 Ω). The lower J with MEAs employing 5 or 30 % Nafion loading is possibly assigned to the higher resistances of the MEAs. MEAs characterized with 10 to 20 wt% of Nafion loading to the Ag amount showed similar FE_{CO}, more than 80% between 2.0 and 2.3 V. At 10 wt% of the optimal Nafion content, we achieved FE_{CO}=97% at 2.3 V and J=100 mA/cm^2 (Figures S6b and S7a).

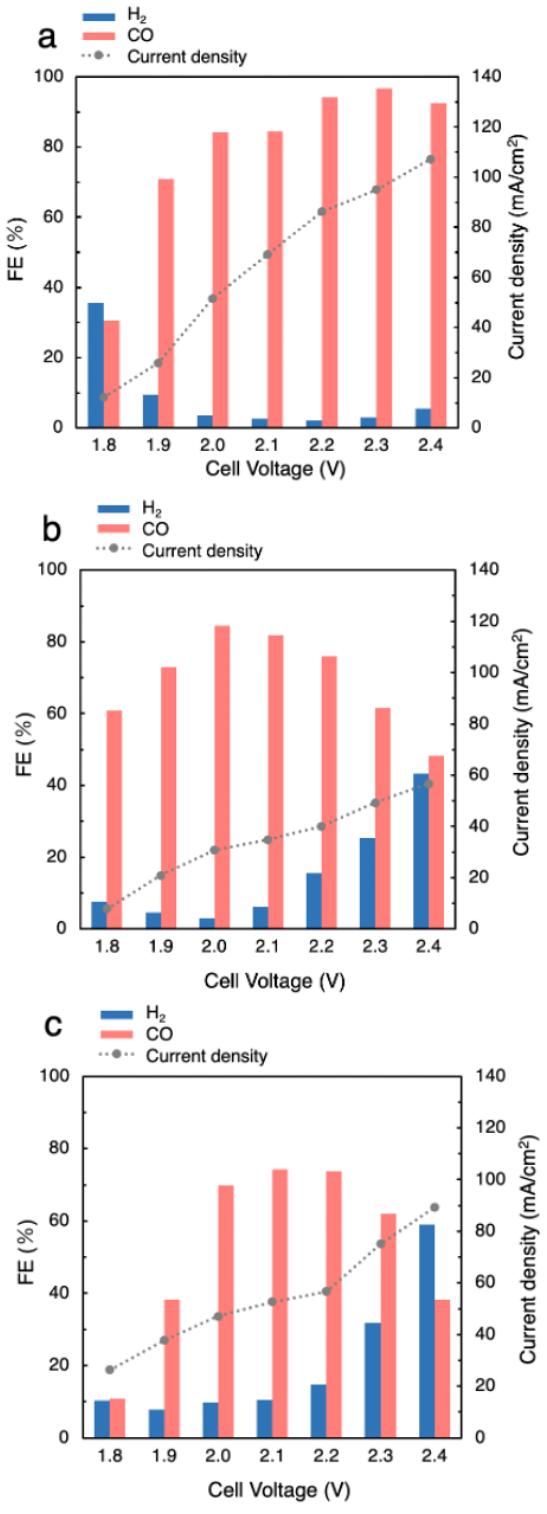

Figure S8. Faradaic efficiency (FE) and current density in CO_2RR using (a) 100% CO_2, (b) N_2-CO_2 and (c) Air-CO_2 on Ag MEA-Cell with10% Nafion loading MEA.

Table S3. Comparison of total current density (J), partial current density (J_{CO}) and FE_{CO} for CO production in state-of-the-art CO_2RR using BCS combined CCU systems.

Feedstock	Catalyst	Membrane	FEco	J (mA/cm^2)	J_{co} (mA/cm^2)	Ref
Sat. CO_2 gas 1.0 M KOH	Ag	CEM	>99%	73	73	This work
Sat. CO_2 gas 1.0 M KOH	Ag	CEM	93%	105	97	This work
2M $KHCO_3$	Ag	CEM	99%	52	51	This work
3M $KHCO_3$	Ag	BPM	62%	200	124	S1
3M $KHCO_3$	Ag	BPM	82%	100	82	S1
3M $KHCO_3$	Ag	BPM	59%	100	59	S2
Sat. N_2 gas 3.0 M $KHCO_3$	Ag	BPM	37%	100	37	S3
Sat. CO_2 gas 3.0 M $KHCO_3$	Ag	BPM	35%	100	35	S3
1.25 M HCO_3^-	Ag	CEM	18%	104	19	S4

References

S1 E. W. Lees, M. Goldman, A. G. Fink, D. J. Dvorak, D. A. Salvatore, Z. Zhang, N. W. X. Loo, C. P. Berlinguette, *ACS Energy Lett.*, 2020, **5**, 2165–2173.

S2 Z. Zhang, E.W. Lees, F. Habibzadeh, D. A. Salvatore, S. Ren, G. L. Simpson, D. G. Wheeler, A. Liu, C. P. Berlinguette, *Energy Environ. Sci.*, 2022, **15**, 705–713.

S3 T. Li, E. W. Lees, M. Goldman, D. A. Salvatore, D. M. Weekes, C. P. Berlinguette, *Joule*, 2019, **3**, 1487–1497.

S4 L. A. Diaz, N. Gao, B. Adhikari, T. E. Lister, E. J. Dufek, A. D. Wilson, *Green Chem.*, 2018, **20**, 620–626.